GEOPHYSICAL RESEARCH LETTERS, VOL. 27, NO. 8, PAGES 1083-1086, APRIL 15, 2000

Homologous sudden disappearances of transequatorial interconnecting loops in the solar corona

Josef I. Khan

Mullard Space Science Laboratory, University College London, Holmbury Saint Mary, Surrey, U.K.

Hugh S. Hudson

Solar Physics Research Corporation, Tucson, Arizona

Abstract. We have found a remarkable sequence of homologous *disappearances* of transequatorial X-ray loops linking active regions. Each disappearance was closely associated with a major flare and coronal mass ejection (CME). In each case the flarings precede the disappearances and the CMEs. Mass estimates for the X-ray loops are similar to CME masses. This, the timing of the disappearances, their morphology, and the homology of the events in the sequence, provide direct evidence for a new class of CME origins in the low corona. We also briefly report observations of features which we infer to be the soft X-ray counterparts of shock waves emanating from the flare region. The inferred shocks appeared to play a vital role in the disappearances. Our results suggest that flare-generated shock waves may destabilize large transequatorial loops, causing them to erupt.

Introduction

Skylab observations revealed that active regions are sometimes connected to each other by magnetic loops much larger than active region structures [*Švestka et al.*, 1977]. Sometimes interconnecting loops are observed to join regions across the solar equator. These transequatorial interconnecting loops are among the largest coronal loops seen in soft X-rays. The existence of very long loops connecting active regions has long been inferred from radio data [*Wild et al.*, 1963; *Stewart and Vorpahl*, 1977]. Their existence has been confirmed by more recent soft X-ray data [*Tsuneta*, 1996].

A full description of interconnecting loops is beyond the scope of this *Letter*. We simply remark that there are many outstanding questions relating to interconnecting loops, such as whether these structures enable interactions between distant active regions (including sympathetic flaring), their relation to active region evolution, how they form, disappear, and 'revive', and whether their disappearances are related to flaring and coronal mass ejections (CMEs). We address the latter point in this work, which also relates to the debate on the causal relation between CMEs and flares.

In this *Letter* we describe a homologous sequence of disappearances of transequatorial interconnecting soft X-ray loops, hereafter simply referred to as 'disappearances', associated with major eruptive flares and CMEs. We use soft X-ray images from the *Yohkoh* Soft X-ray Telescope (SXT) [*Tsuneta et al.*, 1991] to identify the interconnecting loops and examine their general behavior. The spatially unresolved soft X-ray fluxes from the *GOES 9* satellite and radio spectrograms from the Communications Research Laboratory (CRL), Japan are also used as context data.

Paper number 1999GL010730.
0094-8276/00/1999GL010730$05.00

Observations

The interconnecting loops examined here were observed in SXT full-frame images (FFIs) to connect the peripheries of NOAA sunspot region 8214 in the northern hemisphere with region 8210 in the south. Movies of SXT FFIs reveal a remarkable series of *disappearances* of these loops, each closely associated with a major flare in region 8210, a CME, and a type II radio burst.

Each row in Figure 1 shows portions of FFIs before and after each disappearance, and the positive values of the difference of these images. Ignoring features due to solar rotation and in the active regions, the figure clearly demonstrates the disappearances of the interconnecting loops.

During flares the SXT normally switches to a special flare-mode, in which only partial-frame images (PFIs) (but no FFIs) are taken. This has confused the study of flare-CME associations [*Hudson and Webb*, 1997]. In the present context, this reduced data coverage means that we do not directly observe the disappearances of the entire interconnecting loops. Nonetheless, the widest-field-of-view PFIs show portions of these loops which allow us to estimate the intervals during which the disappearances occurred adequately for our purposes.

Table 1 gives the dates for each disappearance and various times, which are self-explanatory. The flares most closely associated with events 1, 2, and 3 were of *GOES* X-ray classes X2.7, M3.1, and M7.7, respectively. The general soft X-ray and temporal context in which the disappearances occurred is presented in Figure 2 which shows the *GOES* soft X-ray flux for times near each disappearance. We will discuss the times shown in Table 1 as we deal with each in turn.

The thick solid vertical lines in Fig. 2 represent the intervals during which the disappearances occurred from inspection of the FFIs alone. To better determine the timing relation of these disappearances with the flares and CMEs we examined the PFIs throughout the intervals shown in Fig. 2. During each of the flares mentioned above, the PFIs were only of region 8210, while before and after the flares PFIs were taken of both regions 8210 and 8214. In the PFIs during the flares a depletion or dimming becomes apparent when we examine differences of images with an early image.

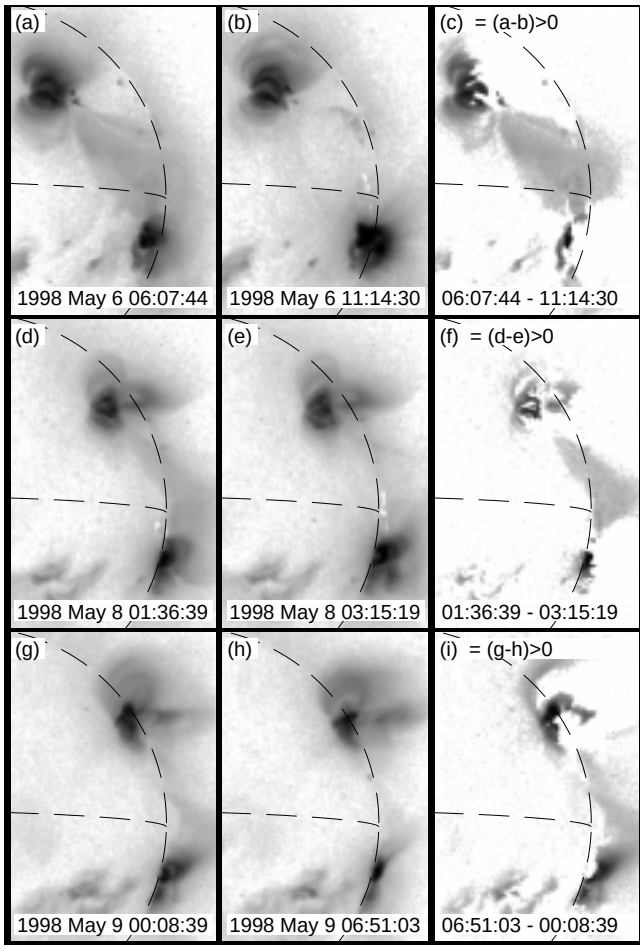

Figure 1. The first two images in each row are portions of SXT FFIs before and after each disappearance. These are scaled (showing relative differences between related images for each event) logarithmically (to exaggerate the apparent brightness of the fainter features) and displayed with a reverse color table where dark represents high intensity (similarly for all figures throughout). The third image in each row is the difference of the first two images but with only the positive values of the difference shown and scaled to span the full range of display values available.

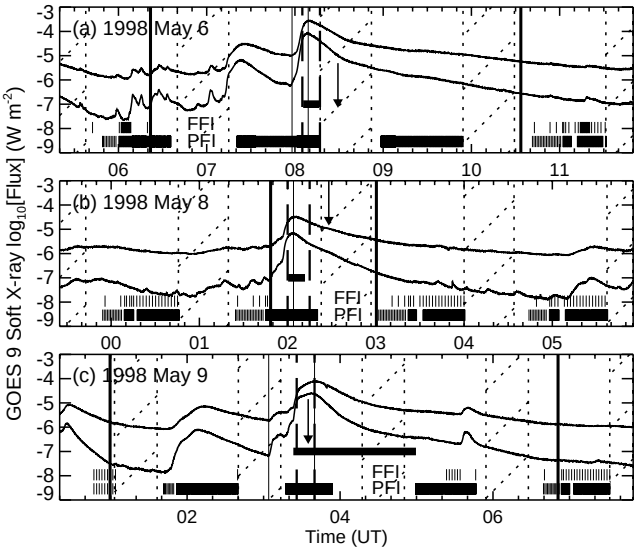

Figure 2. The soft X-ray flux from the *GOES 9* low (∼1–8 Å, the higher flux curve) and high (∼0.5–4 Å) energy channels for each disappearing interconnecting loop event. Superimposed on these are hatched areas representing the intervals of *Yohkoh* satellite night and small vertical tick marks indicating the times of SXT FFIs (upper bands) and PFIs (lower bands). Other superposed features are discussed in the main text.

Near the time of disappearance event 1 there were two major flares (*GOES* X-ray class M2.9, maximum at 07:25, and X2.7 at 08:09). The PFIs show that the disappearance was related to the second of these flares. The first row (labeled (a)) of Figure 3 shows a portion of a direct image for each event; subsequent rows are differences relative to these frames. Each column represents a different disappearance event. Because of the relatively long exposure durations and the high activity, the images show saturation (set to zero, and thus these appear white in the figure) of the SXT CCD over active region 8210. The first several difference images in rows (b)–(e) are of images before and during the (soft X-ray) rise of the flares. In some of these images outward moving soft X-ray features associated with the flare are seen (whose edges are indicated by open-headed arrows). At the time of the images in row (f) the outward moving features appear to cross the vicinity of the southern footpoints of the interconnecting loops. During the flares the saturation increases and takes the form of vertical streaks in the CCD; there is also increased scattering throughout the images. As the scattered intensity from the flare drops we observe depleted regions which we infer to be due to the disappearances. We infer the disappearances occurred between the interval for the images shown in rows (f) and (g). These intervals are indicated by horizontal bars on Fig. 2 and listed in Table 1. Images in row (h) are for later times which shows the depletions more clearly. For event 3, the early images include structures which are already (repeatedly) flaring. The difference images for event 3 therefore show depletions due to the changes in the earlier flare. These are quite distinct from those seen later, which are clearly related to the disappearance. The estimated time of disappearance for event 3 is relatively long compared to the others because there is a gap in the data coverage from 03:53:45 (which still shows strong

Table 1. Disappearing Interconnecting Loop Events in 1998 May

No.	Day	Loops in FFIs		Disappearance of	*GOES* Flare		HiRAS Type II	SXT Wave	HXT Burst
		Last Seen	Not Seen	Loops in PFIs	Start	Peak	Time Interval	Start	Start
1	6	06:21:46	10:33:34	08:05:34–08:16:26	07:58	08:09	08:05–08:17	08:03:36	08:01:20
2	8	01:48:25	03:00:23	02:00:21–02:11:29	01:49	02:04	02:00–02:15	01:59:27	01:56:50
3	9	00:59:33	06:51:03	03:23:21–04:59:35	03:04	03:40	03:26–03:40	03:19:45	03:18:52

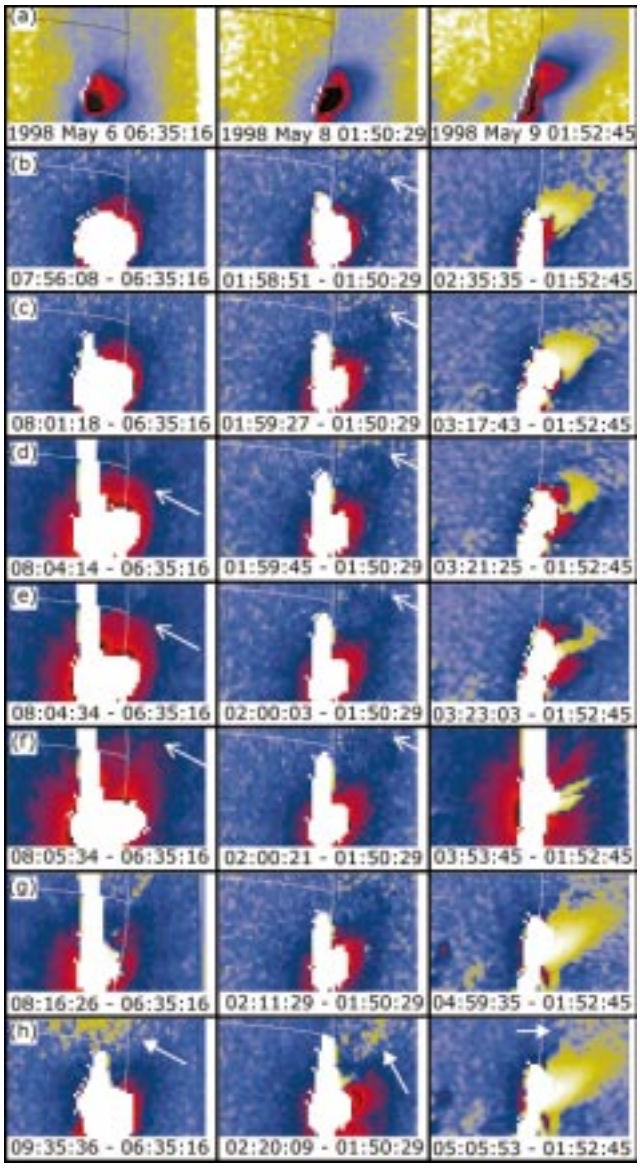

Figure 3. The first images in each column show portions of SXT PFIs before each interconnecting loop disappearance event. Subsequent images in each column show difference images scaled logarithmically. The open-headed arrows show the inferred edge of the SXT waves, while the closed-headed arrows show the inferred disappearance of the interconnecting loops. Yellow indicates a depletion in the difference images. See the main text for a full description.

scattering) until 04:59:35 (which shows the disappearance clearly).

Hiraiso radio spectrograph (HiRAS) data from CRL presented in Figure 4 show that the flares related to each disappearance are associated with metric type II, III, and IV bursts. Of most interest here are the type II bursts, which are generally associated with shock waves. All of the flares associated with each disappearance show outward moving features from the flare region shortly after the flare start in the SXT PFIs. We estimate the speed of these moving features $\approx$770–900 km s^{-1}. The speeds, morphology and timing relative to the type II bursts, lead us to conclude that these features may be the soft X-ray counterparts of a coronal shock wave seen in SXT images for the first time, analogous to those observed by the Solar and Heliospheric Observatory (SOHO) Extreme Ultraviolet Imaging Telescope (EIT) [*Thompson et al.*, 1998] and, of course, as type II bursts (cf. [*Klein et al.*, 1999] who described moving loops as the drivers of a shock wave). The association of the moving soft X-ray features with coronal shock waves is tentative; detailed analysis providing evidence of this interpretation, including EIT observations, will be presented elsewhere [*Hudson et al.*, 2000]. The estimated times of first appearance of the outward moving soft X-ray features in the widest-field-of-view PFIs are given in the second-last column in Table 1. The interval for which type II bursts are seen in the HiRAS data (long-dashed vertical lines in Fig. 2) are also given in the table. Thin vertical lines in Fig. 2 show the soft X-ray flare start and peak for each event, clearly demonstrating that the soft X-ray flare starts before the type II bursts, the SXT wave, and the disappearance. Examination of hard X-ray data from the *Yohkoh* Hard X-ray Telescope (HXT) [*Kosugi et al.*, 1991] also confirm that the soft X-ray flare starts first for each event. The last column in Table 1 gives the start time of the HXT M2 channel bursts.

LASCO C2 coronagraph [*Brueckner et al.*, 1995] images first show loop-like CMEs associated with disappearance events 1–3 at the times 08:29, 02:28, and 03:36 on their respective days (times indicated by arrows in Fig. 2). Each column in Figure 5 represents a different disappearance event. The first row, (a), shows difference images when the first loop-like CMEs were seen, while (b) shows difference images at later times.

Using SXT filter ratios [*Tsuneta et al.*, 1991] we calculated a temperature, T, and emission measure, EM, (in the isothermal approximation) of the interconnecting loop prior to the May 6 disappearance. This was done both by integrating parameter maps made with the full pixelization ($4.9''$) via averaging, and via obtaining total signals for the whole interconnecting loop prior to the parameter estimation. Both methods agreed on $T\approx4$ MK and $EM\approx10^{47}$ cm^{-3}. The length of the interconnecting loop, $s_1\approx5\times10^8$ m, while the maximum width near the loop-top region, $s_2\approx2\times10^8$ m. Assuming an approximate emitting volume given by $s_1(s_2/2)^2$ results in a mass estimate of the interconnecting loop of $\approx10^{15}$ g, close to currently accepted values for CME masses.

Discussion

In this work we have presented evidence of a category of CMEs, not been reported previously, which is new in terms of the low-coronal origins and the inferred mechanism by which the CME occurs. These CMEs are closely associated with disappearing transequatorial interconnecting loops (whereas in other cases the CME origin is more closely associated with erupting filaments or structures above flaring arcades either inside or outside of active regions). The observations were of a series of three successive disappearing transequatorial interconnecting loops which were homologous in the sense that the disappearing structures strongly resembled each other in form and location prior to the disappearance, as well as timing relative to the flares (and the behavior of the flares themselves).

These results partly confirm the general appearance noted by [*Harrison*, 1995] that a CME can be occur non-concentrically with its associated flare. However our results show the flare may not occur along the CME structure, but out-

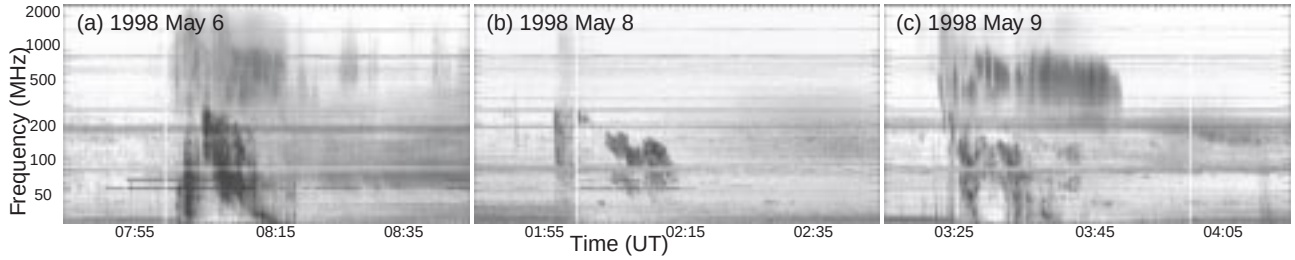

Figure 4. HiRAS radio spectrograms showing that the flares related to each disappearance are associated with metric type II (and other) bursts.

side of it. The CME structures appear above the locations of the interconnecting loops, not the flaring arcades. The present work also shows that the mass of the interconnecting loop structure may be comparable to that of a major CME. This, the timing of the disappearances of the interconnecting loops relative to the CMEs, the morphological similarities between these structures, and the similarities in behavior for all three events lead us to conclude that the soft X-ray images show the CME material prior to its ejection. We find that in all cases the flare closely associated with each disappearance starts (as defined by hard or soft X-ray emission) before the interval during which the disappearance occurred. Each flare shows outward moving soft X-ray features whose speeds, morphology, and timing relative to metric type II bursts suggests that they may be the soft X-ray counterparts of coronal shock waves seen for the first time in the SXT data. We suggest that the inferred shock waves may have played a crucial role in the disappearances of interconnecting loops. The data show that for each case the disappearance (and inferred ejection) of the interconnecting loop follows the passage of large-scale shock waves launched from an active region at one end of the structure.

Perhaps the most important clarification made possible by these observations is the heretofore controversial timing relationship between the flare process and the CME. We find that ejections launched on compact scales [*Klein et al.*, 1999] can precede the associated CME. There is now clear evidence that shock waves associated with flaring activity may destabilize large-scale structures which produce some CMEs.

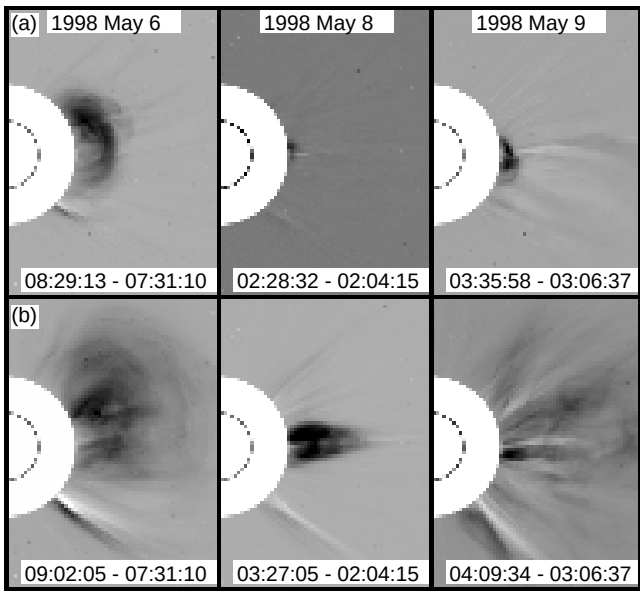

Figure 5. SOHO LASCO C2 difference images for each disappearance event (in separate columns).

Acknowledgments. The *Yohkoh* mission is a project of the Institute of Space and Astronautical Science (ISAS) of Japan. It is financially supported by ISAS, NASA, and the Particle Physics and Astronomy Research Council (PPARC) of the UK. We thank S. Nagai of the Hiraiso Solar Terrestrial Research Center, CRL, Japan for preparing and providing the radio spectrograms. We are grateful to the SOHO LASCO Team for providing data and software. J.I.K. received support from PPARC. H.S.H was supported under NASA contract NAS 8-40801.

References

Brueckner G. E., et al., The Large Angle Spectroscopic Coronagraph (LASCO), *Solar Phys., 162,* 357–402, 1995

Harrison, R., The nature of solar flares associated with coronal mass ejections, *A&A, 304,* 585–595, 1995

Hudson H. S., and D. F. Webb, Soft X-ray signatures of coronal ejections, in Geophysical Monograph #99, *Coronal Mass Ejections: Causes and Consequences,* edited by N. Crooker, J. A. Joselyn, and J. Feynman, American Geophysical Union, Washington, D.C., pp. 27–38, 1997

Hudson H. S., et al., Soft X-ray observations of a large-scale coronal wave and its exciter, In preparation. To be submitted to *Astrophys. J.*

Klein K.-L, et al., X-ray and radio evidence on the origin of a coronal shock wave, *A&A, 346,* L53–L56, 1999

Kosugi T., et al., The Hard X-ray Telescope (HXT) for the Solar-A mission, *Solar Phys., 136,* 17–36, 1991

Stewart R. T., and J. Vorpahl, Radio and soft X-ray evidence for dense non-potential magnetic flux tubes in the solar corona, *Solar Phys., 55,* 111–120, 1977

Švestka Z., et al., Transequatorial loops interconnecting McMath regions 12472 and 12474, *Solar Phys.,* 52, 69–90, 1977

Thompson B. J., et al., SOHO EIT observations of an Earth-directed coronal mass ejection on May 12 1997, *Geophys. Res. Lett., 25,* 2461–2464, 1998

Tsuneta S., et al., The Soft X-ray Telescope for the Solar-A mission, *Solar Phys., 136,* 37–67, 1991

Tsuneta S., Interacting active regions in the solar corona, *Astrophys. J., 456,* L63–L65, 1996

Wild J. P., S. F. Smerd, and A. A. Weiss, Solar bursts, *ARA&A, 1,* 291, 1963

J. I. Khan and H. S. Hudson, *Yohkoh* Data Analysis Center, Institute of Space & Astronautical Science, 3-1-1 Yoshinodai, Sagamihara, Kanagawa 229-8510, Japan. (e-mail: jkhan@solar.stanford.edu; hhudson@solar.stanford.edu)

(Received September 10, 1999; revised December 5, 1999; accepted December 28, 2000.)